Spatiotemporal structure of complex cell receptive fields and influence of GABAergic inhibition

Sheng Liu[a,b], Yong-Jun Liu[a] and Bing Li[a]

[a]State Key Laboratory of Brain and Cognitive Science, Institute of Biophysics, Chinese Academy of Sciences, and [b]Graduate School of the Chinese Academy of Sciences, Beijing, PR China

Correspondence to Dr Bing Li, Institute of Biophysics, Chinese Academy of Sciences, Beijing 100101, PR China
Tel: +86 10 6488 8529; fax: +86 10 6485 3625; e-mail: lib@sun5.ibp.ac.cn

Received 15 May 2007; accepted 1 June 2007

Spatiotemporal receptive field (RF) profiles were mapped with reverse correlation technique for complex cells in the striate cortex of cat. The RFs were constituted with ON and OFF subfields that overlapped much extensively in space and also largely in time. The subfields had spatial width of 1.0–4.3° and temporal duration of 33–139 ms, whereas late responses were absent in most cases. When microiontophoresis of γ-aminobutyric acid type A ($GABA_A$) antagonist bicuculline was performed on the cells, little change occurred in width and onset time of the subfields, but the duration was prolonged in a subset of cells. These results suggest that intracortical inhibition may contribute to improve the accuracy of visual signals encoded in neuronal activities, but is unlikely critical for determining the primary structure of complex cell RF. *NeuroReport* 18:1577–1581 © 2007 Wolters Kluwer Health | Lippincott Williams & Wilkins.

Keywords: bicuculline, complex cell, GABAergic inhibition, receptive field, spatiotemporal properties, striate cortex

Introduction

The receptive field (RF) is defined classically as the area of visual space within which the discharge of a neuron can be influenced. In the striate cortex, two primary RF configurations are distinguished by whether the ON and OFF subfields are superimposed or not, and attributed to simple and complex cells, respectively [1,2]. Although much attention has been focused on the spatial structure, the RF is inherently a spatiotemporal entity as it often exhibits striking dynamics along the time [3–6]. With various mapping techniques (in particular the reverse correlation analysis), the spatiotemporal RF dynamics are extensively investigated for simple cells [7–12] but not as much for complex cells [13–15]. Thus far, the quantitative description of spatiotemporal characteristics of complex cell RFs remains insufficient.

The conformation of RF structure is a central concern in visual neurophysiology. It is generally agreed that simple cells are created from the convergence of thalamic inputs with RFs aligned in visual space and complex cells are, in turn, generated by pooling the inputs from simple cells with similar orientation preferences (however, a minority of complex cells may have their RFs constructed from direct geniculate inputs) [1,16]. In addition, local intracortical circuits play an important role in sculpturing the RF structure and modulating the stimulus selectivity of the cell [16,17]. Specifically, previous studies have shown that blockade of the GABAergic inhibition may change the RF structures of striate neurons [18–22]; nevertheless, more detailed data are necessary for a comprehensive understanding of this matter. This study combined the reverse correlation technique for dynamic RF mapping with microiontophoresis of $GABA_A$ antagonist bicuculline to investigate the contribution of local inhibitory mechanism to the spatiotemporal RF properties of complex cells in cat striate cortex.

Methods

Experiments were carried out on six normal adult cats, approved by the Animal Ethical Committee of our institution. The detailed procedures for animal preparation and maintenance have been described previously [23]. Adequate measures (anesthesia and paralysis, continuous monitoring of physiological conditions, protection of eyes, and so on) were taken to minimize pain and discomfort of the cats, in compliance with the National Institutes of Health guidelines on the care and use of laboratory animals. Single-unit recordings and microiontophoresis were performed in the striate cortex (area 17) with triple-barreled glass pipettes (total tip diameter approximately 6–9 μm, resistance of single barrel approximately 20–30 MΩ). The recording barrel was filled with 0.5 M sodium acetate containing 4% pontamine skyblue (for histological identification of the recording site), the drug barrel was filled with bicuculline methiodide (5 mM in 150 mM NaCl, pH 3.5; Sigma, St Louis, Missouri, USA), and the third barrel was filled with 0.9% NaCl (pH 3.5) for balancing the current. The current for bicuculline injection was in the range between +20 and +30 nA (retaining current −15 nA). The effects were examined after bicuculline had been administered for 5 min.

Before the microiontophoresis, the RF of a single cell was approximately plotted with hand-held stimuli and was classified as simple or complex according to the conven-

tional criteria [1] or by a quantitative test [24]. In further study, the spatiotemporal RF profile was mapped with the reverse correlation technique (for the algorithm and detailed procedures see Refs. [4,5,8]). To elicit sufficient visual responses and reduce the time consumption, one-dimensional (1-D) mapping was performed with elongated thin bars (typically 10° in length and 0.5° in width). Stationary bright (32 cd/m^2) and dark (2 cd/m^2) bars of optimal orientation were displayed one at a time to the dominant eye on a background of intermediate luminance (17 cd/m^2) at 20 locations across a stimulus patch. The patch (normally 10° in width) was positioned to cover the entire RF and its surrounding area. The 40 different stimuli (20 locations × 2 contrast polarities, appearing for 40 ms each) were pseudo-randomly interleaved to compose a trial. After an interval of 1–2 s, the stimulus sequence was rerandomized and presented again. The procedure was repeated for 50–100 trials to complete a recording.

In data analysis, a pair of firing rate matrices (corresponding to bright and dark stimuli, respectively) were constructed by computing the spatial profiles of neuronal activity for a series of time delays (T=0, 10, 20, ..., 200 ms). For each T value, the recorded spike train was reparalleled with the stimulus sequence, and the activity correlated to a certain stimulus could be determined by summarizing the number of spikes within a 20-ms time window starting T ms after the onset of the stimulus. The matrices were illustrated as x–t plots to show the spatiotemporal organization of ON and OFF subfields (see examples in Fig. 1). For each x–t plot, the data (originally in a resolution of 0.5° in space and 10 ms in time) were subjected to a linear interpolation without any smoothing or filtering, and the outcome was drawn as an isoamplitude contour map. The background activity was estimated by averaging the discharge rates recorded during visual stimulation at two remote locations outside the RF, the mean was subtracted from all activity values, and the standard error was used to set a threshold for evoked responses (i.e. the baseline in contour map). The subfield was characterized in terms of width and duration, obtained by measuring the maximal spatial and temporal ranges of the region displaying distinct responses. Moreover, an overlap index was calculated as: $OI=(0.5W_{ON}+0.5W_{OFF}-d)/(0.5W_{ON}+0.5W_{OFF}+d)$, where W_{ON} and W_{OFF} were the widths of the ON and OFF subfields and d was the distance between the central positions of the two subfields [16,17].

Results

The spatiotemporal RF profiles (x–t plots) were successfully obtained and analyzed for 17 complex cells. The cells were orientation selective to bar and grating. Similar to the two examples shown in Fig. 1, all the cells exhibited one ON and one OFF subfields which overlapped much extensively in space (OI averaged at 0.80±0.15) and also largely in time. Normally, a subfield appeared as a continuum in the spatiotemporal map, except that in a few cases some kind of late responses were observed (see Fig. 1b). Primary responses usually began at about 15–35 ms after stimulus onset and lasted for no more than 100 ms. During the period, the spatial range of a subfield could be somewhat variable with time, but the spatial position displaying optimal responses was relatively stable and thus the elongated subfield was oriented approximately parallel to the t-axis of x–t plot.

Table 1 summarizes the statistics on spatial and temporal characteristics of the ON/OFF subfields and the overall RF. Concretely, the spatial width ranged from 1.0 to 4.0° for ON subfields and from 1.3 to 4.3° for OFF subfields. As for the temporal duration, the range was 33–84 and 37–139 ms, respectively. The overall RF of a cell was considered as the

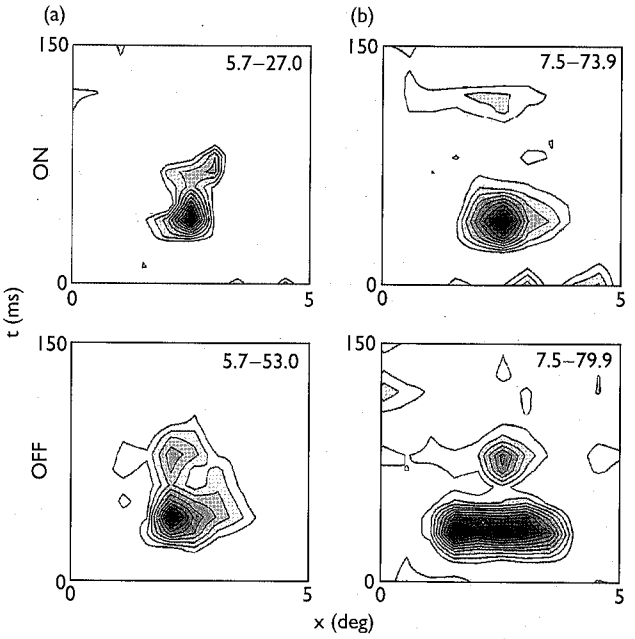

Fig. 1 Spatiotemporal RF profiles of two complex cells. The regions displaying different levels of evoked responses are outlined by a series of isoamplitude contours. The baseline threshold is determined upon the mean background activity and its standard error (see Methods), and the discharge strength is coded in a grey scale ranging linearly from the threshold to the maximal response value (the practical range is given individually in each panel in spikes/sec). (a) ON and OFF subfields were superimposed not only in the spatial, but also in the temporal domain. (b) The subfields overlapped in space and in early phase of time (up to approximately 60 ms after stimulus onset). Late responses were pronounced for OFF but not firmly conclusive for ON subfield.

Table 1 Spatial width, temporal duration and onset time (mean±SD) of ON/OFF subfields and overall RFs in normal condition and during bicuculline application (Bicu)

	Normal (n=17)			Bicu (n=14)		
	Width (°)	Duration (ms)	Onset (ms)	Width (°)	Duration (ms)	Onset (ms)
ON subfield	1.9±0.9	52±15	32±12	1.9±0.7	63±22	32±15
OFF subfield	2.5±0.8	67±26	22±13	2.6±0.8	77±33	24±17
Overall RF	2.6±0.9	79±23	19±8	2.7±0.8	90±34	19±13

Bicu, bicuculline; RF, receptive field.

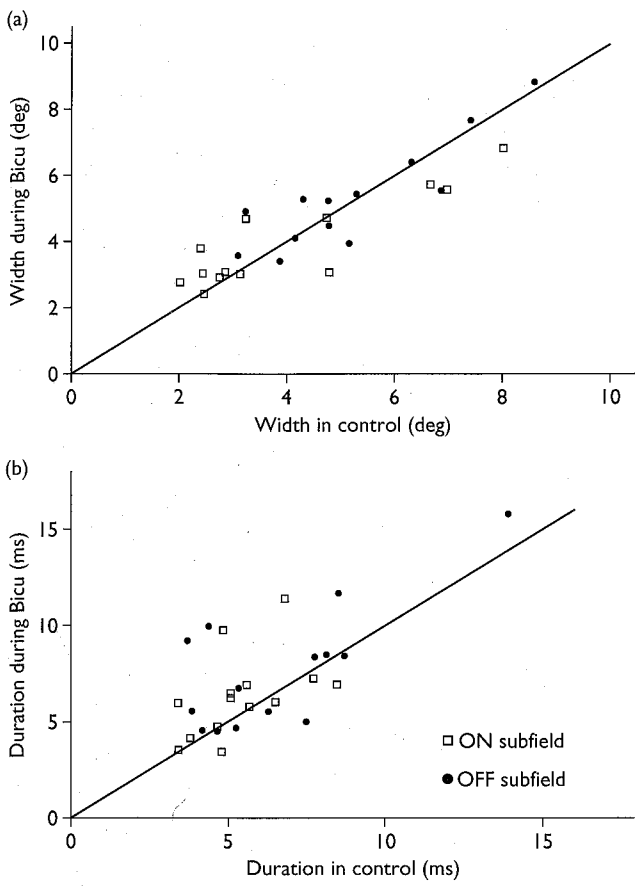

Fig. 2 Scatter plots showing the effect of bicuculline application on spatial width (a) and temporal duration (b) of ON and OFF subfields. The difference between the control and Bicu data was in a negligible quantity for width (2.2 ± 0.9 vs. 2.2 ± 0.8, ON and OFF data were pooled) but became moderate for duration (60 ± 23 vs. 70 ± 28, Wilcoxon test, $P < 0.05$).

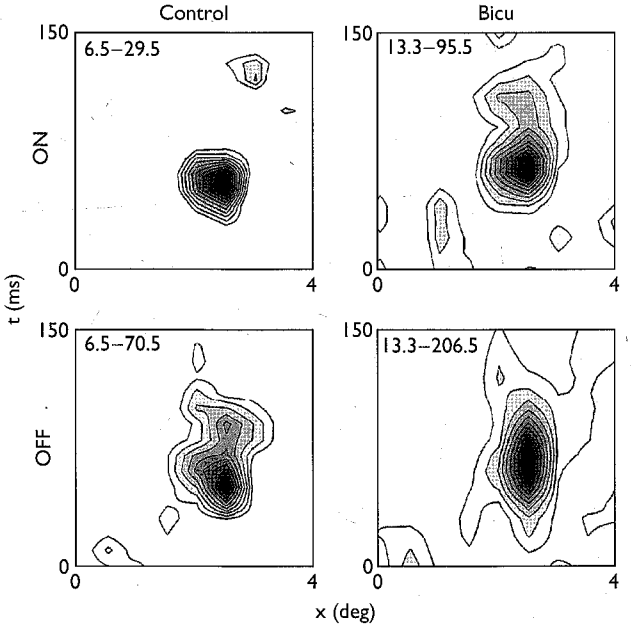

Fig. 3 Spatiotemporal RF profiles of a complex cell before and during bicuculline application. The change of spatial width was small: from 1.2 to 1.5° for ON and from 1.5 to 1.8° for OFF subfield. On the contrary, the prolongation of temporal duration was dramatic: from 48 to 97 ms and from 85 to 116 ms, respectively.

combination of its subfields; however, the size was only slightly larger either in the spatial (1.4–4.5°) or in the temporal (42–139 ms) domain, as the subfields were substantially superimposed.

Consistent with the results described in the literature, the application of bicuculline typically increased the neuronal responses to visual stimuli and the background activities, and the effects were recoverable after the microiontophoresis. The spatiotemporal RF profiles of most cells, however, did not exhibit any remarkable alteration. As shown in Table 1 and Fig. 2a, little change occurred in width and onset time of either ON or OFF subfields. The situation for temporal duration was somewhat different that obvious prolongation was observed in a subset of cells (see Fig. 3) whereas almost none displayed clear shortening (as shown in Fig. 2b, seven out of 28 subfields had the duration increased by 37–149%, the largest decrease was −34%). No relationship was found between RF variation and recording site of the cells. Finally, examination on the locations of ON/OFF subfields did not show any systematic shift in either space or time, or any significant change in the extent of subfield superimposition (OI 0.81 ± 0.14 vs. 0.87 ± 0.07, Wilcoxon test, $P > 0.15$).

Discussion

The approach of reverse correlation analysis used in this study has been applied mostly to simple cells but only occasionally to complex cells, therefore the comparable data are rarely available in the literature. This may be partly because the so-called first-order RF profiles obtained with this approach have little power for providing accurate predictions of the nonlinear response properties of a complex cell [3,13,14]. Nevertheless, these profiles define the spatiotemporal envelope of the RF and should be useful for characterizing the RF quantitatively and describing its variation under manipulation (e.g. the blockade of intracortical inhibition).

The spatiotemporal RF envelopes we observed were obviously smaller than those obtained from area 18 complex cells [5], and also smaller than area 17 simple cells in the temporal domain [8]. Besides the inherent differences between the areas or the cell types, the methodological consideration in data analysis should be addressed. First, although not clearly interpreted in Ref. [5], it looks as if the mean background activity was taken as the threshold for determining the occurrence of visual responses in the spatiotemporal map. Alternatively, we used a more stringent criterion (see Methods and Fig. 1), which would result in smaller RF size. Second, the Gaussian filtering, which removes or reduces high frequency components in data, was often performed to smooth the data of RF mapping [4,6,8,11]. The high frequency components, however, are not simply noise but also come from dramatically varying signals (specifically in the case that the visual responses at RF center are much higher above the spontaneous activity). Thus the smoothing may lead to an overestimation of bandwidth, especially when the tuning is sharp. Usually, the blockade of GABAergic inhibition highly increases the visual responses but the effect on spontaneous activity is less pronounced, as a result, the RF profile would become sharper. Therefore we did not apply any smoothing or filtering in data analysis to avoid the potential systematic error.

The temporal characteristics are a major issue in relevant RF mapping experiments. In a representative study on area 17 simple cells, the peak response time averaged at 68.2 ms and the duration at 139.6 ms [8]. Much differently, Gonzalez and coworkers [6] reported RF onset time of 51.3 ms and duration of 32.7 ms for macaque V1 cells (cell type not classified). In our results, the mean duration was 79 ms with RF onset at ~20 ms and peak response at 55–60 ms. These differences seem striking but are unlikely a reality in the striate cortex. The criterion for defining a RF structure might be overcareful in Ref. [6], so that the onset time was late and the duration was short. The simple cell RFs were analyzed in a different way in Ref. [8] (see Fig. 6 and the context); nevertheless, the separation of ON and OFF responses in the temporal domain might contribute substantially to the long duration.

Generally, the RF properties we observed are consistent with the normal understanding about area 17 complex cells, but different from the results obtained in area 18 with a comparable approach [5]. The difference in spatial width was explained by the larger eccentricity of area 18 recordings and the generally larger RF size of area 18 cells [5]. On the other hand, the longer temporal duration of area 18 cells should be mainly due to the frequent appearance of late responses (see Fig. 6 in Ref. [5]). On the contrary, the definite late responses were rarely seen in our sample, indicating that there might be some kind of regional difference between the two areas. Additionally, the inherent difference could be amplified by the methodological consideration in data analysis (see above) and stimulus setting Ref. (see Discussion in Ref. [5]).

The effects of bicuculline application on spatiotemporal RF characteristics were not remarkable in our experiments, except for the prolongation of duration in a subset of cells. Pernberg and co-workers [5] reported seemingly very different findings that the blockade of local inhibition in area 18 widened RF subfields in space and shortened the response duration in time. The spatial enlargement of subfields, however, was distinct for simple cells but insignificant for complex cells. In the temporal domain, the decrease of duration mostly resulted from the shortening or even loss of late responses (see Fig. 6 in Ref. [5]), which were often absent in our sample. Actually, the mean duration under the action of bicuculline (97 ms in Ref. [5]) was only slightly longer than ours (90 ms), also suggesting that the difference between the two areas is dominated by the late responses.

Previous studies on the contribution of GABAergic inhibition to RF structures of striate neurons have shown that, during the application of bicuculline, ON and OFF subfields of simple cells become less isolated or even superimposed, but in complex cells only the relative strengths of the subfields are changed [18,20,21]. Our results also indicate that intracortical inhibition is probably not critical for determining the primary structure of complex cell RF. On the other hand, it is widely agreed that the local inhibitory mechanism can enhance the functional specificity of cortical cells (e.g. modulating the orientation, direction and length preferences; see Refs. [17,18,21,22]). Conceivably, it may contribute to improve the accuracy of visual signals encoded in neuronal activities. The alteration of RF duration in the present study (tending to be prolonged by bicuculline) is consistent with the hypothesis on the role that GABAergic inhibition may play in cortical processing.

Conclusion

This study provided a quantitative description about RF structures of complex cells in cat striate cortex, in terms of spatial width, temporal duration and onset time. These properties exhibited little change under the action of bicuculline, except for the prolongation of duration in a subset of cells. These results may help to promote the understanding on the contribution of intracortical inhibition to RF structure of complex cell.

Acknowledgements

This work was supported by the National Basic Research Program of China (Grant no. 2005CB724301), the National Natural Science Foundation of China (Grant no. 90408020) and the Knowledge Innovation Program of the Chinese Academy of Sciences (Grant no. KSCX1-YW-R-32).

References

1. Hubel DH, Wiesel TN. Receptive fields, binocular interaction and functional architecture in the cat's visual cortex. *J Physiol (Lond)* 1962; **160**:106–154.
2. Ringach DL. Mapping receptive fields in primary visual cortex. *J Physiol (Lond)* 2004; **558**:717–728.
3. DeAngelis GC, Ohzawa I, Freeman RD. Receptive-field dynamics in the central visual pathways. *Trends Neurosci* 1995; **18**:451–458.
4. Cai D, DeAngelis GC, Freeman RD. Spatiotemporal receptive field organization in the lateral geniculate nucleus of cats and kittens. *J Neurophysiol* 1997; **78**:1045–1061.
5. Pernberg J, Jirmann KU, Eysel UT. Structure and dynamics of receptive fields in the visual cortex of the cat (area 18) and the influence of GABAergic inhibition. *Eur J Neurosci* 1998; **10**:3596–3606.
6. Gonzalez F, Castro AF, Romero MC, Bermudez MA, Perez R. Temporal characteristics of visual receptive fields in primary visual cortex and medial superior temporal cortex areas. *NeuroReport* 2006; **17**:5 65–569.
7. McLean J, Palmer LA. Contribution of linear spatiotemporal receptive field structure to velocity selectivity of simple cells in area 17 of cat. *Vision Res* 1989; **29**:675–679.
8. DeAngelis GC, Ohzawa I, Freeman RD. Spatiotemporal organization of simple-cell receptive fields in the cat's striate cortex. I. General characteristics and postnatal development. *J Neurophysiol* 1993; **69**: 1091–1117.
9. Reid RC, Victor JD, Shapley RM. The use of m-sequences in the analysis of visual neurons: linear receptive field properties. *Vis Neurosci* 1997; **14**:1015–1027.
10. De Valois RL, Cottaris NP, Mahon LE, Elfar SD, Wilson JA. Spatial and temporal receptive fields of geniculate and cortical cells and directional selectivity. *Vision Res* 2000; **40**:3685–3702.
11. Livingstone MS, Conway BR. Contrast affects speed tuning, space-time slant, and receptive-field organization of simple cells in macaque V1. *J Neurophysiol* 2007; **97**:849–857.
12. Malone BJ, Kumar VR, Ringach DL. Dynamics of receptive field size in primary visual cortex. *J Neurophysiol* 2007; **97**:407–414.
13. Emerson RC, Bergen JR, Adelson EH. Directionally selective complex cells and the computation of motion energy in cat visual cortex. *Vision Res* 1992; **32**:203–218.
14. Gaska JP, Jacobson LD, Chen HW, Pollen DA. Space-time spectra of complex cell filters in the macaque monkey: a comparison of results obtained with pseudowhite noise and grating stimuli. *Vis Neurosci* 1994; **11**:805–821.
15. Pack CC, Conway BR, Born RT, Livingstone MS. Spatiotemporal structure of nonlinear subunits in macaque visual cortex. *J Neurosci* 2006; **26**: 893–907.
16. Martinez LM. The generation of receptive-field structure in cat primary visual cortex. *Prog Brain Res* 2006; **154**:73–92.
17. Hirsch JA, Martinez LM. Circuits that build visual cortical receptive fields. *Trends Neurosci* 2006; **29**:30–39.
18. Sillito AM. The contribution of inhibitory mechanisms to the receptive field properties of neurones in the striate cortex of the cat. *J Physiol (Lond)* 1975; **250**:305–329.

19. Wolf W, Hicks TP, Albus K. The contribution of GABA-mediated inhibitory mechanisms to visual response properties of neurons in the kitten's striate cortex. *J Neurosci* 1986; **6**:2779–2795.
20. Eysel UT, Shevelev IA. Time-slice analysis of inhibition in cat striate cortical neurons. *NeuroReport* 1994; **5**:2033–2036.
21. Eysel UT, Shevelev IA, Lazareva NA, Sharaev GA. Orientation tuning and receptive field structure in cat striate neurons during local blockade of intracortical inhibition. *Neuroscience* 1998; **84**:25–36.
22. Murthy A, Humphrey AL. Inhibitory contributions to spatiotemporal receptive-field structure and direction selectivity in simple cells of cat area 17. *J Neurophysiol* 1999; **81**:1212–1224.
23. Xu Y, Li B, Li B-W, Diao Y-C. Adaptation of PMLS neurons to prolonged optic flow stimuli. *NeuroReport* 2001; **12**:4055–4059.
24. Skottun BC, De Valois RL, Grosof DH, Movshon JA, Albrecht DG, Bonds AB. Classifying simple and complex cells on the basis of response modulation. *Vision Res* 1991; **31**:1079–1086.